연구논문

Journal of Drive and Control, Vol.16 No.1 pp.45-53 Mar. 2019
ISSN(print) 2234-8328 ISSN(online) 2287-6146
http://dx.doi.org/10.7839/ksfc.2019.16.1.045

Design, Modeling and Analysis of a PEM Fuel Cell Excavator with Supercapacitor/Battery Hybrid Power Source

Tri Dung Dang[1], Tri Cuong Do[1], Hoai Vu Anh Truong[1], Cong Minh Ho[1], Hoang Vu Dao[1], Yu Ying Xiao[1], EunJin Jeong[1] and Kyoung Kwan Ahn[2*]

Received: 25 Feb. 2019, Accepted: 26 Feb. 2019

Key Words : Hybrid Excavator, PEM Fuel Cell, Supercapacitor, Battery, System Modeling.

Abstract: The objective of this study was to design and model the PEM fuel cell excavator with supercapacitor/battery hybrid power source to increase efficiency as well as eliminate greenhouse gas emission. With this configuration, the system can get rid of the internal combustion engine, which has a low efficiency and high emission. For the analysis and simulation, the governing equations of the PEM system, the supercapacitor and battery were derived. These simulations were performed in MATLAB/Simulink environment. The hydraulic modeling of the excavator was also presented, and its model implemented in AMESim and studied. The whole system model was built in a co-simulation environment, which is a combination of MATLAB/Simulink and AMESim software. The simulation results were presented to show the performance of the system.

Nomenclature

H_2 : Hydrogen

O_2 : Oxygen

H_2O : Water

e^- : Electron

FCS: Fuel cell stack

1. Introduction

Construction excavators play an important role in construction site. Due to the environmental pollution and the lack of fossil fuel, many researches have been focusing on saving energy and reducing emission with respect to construction excavators[1-4]. The internal combustion engine (ICE) excavator has shown low energy efficiency, limited working torque and speed range, noise and a lot of emissions. Thus, ICE type excavator has been recently replaced by the hybrid type[5-14]. Hydraulic hybrids excavators are energy-effective with good power performance and fuel economy[8-14]. However, the excavators are still using an engine which is not 'green' power sources and cannot get rid of the carbon emission. Fuel cell (FC) power sources have shown great performance and become a successful application when applied to fuel cell vehicles[15-17]. Yi et al. suggested that we can replace the traditional diesel/gas ICE by fuel cells system in construction excavator[18]. The advantages of Proton-exchange membrane (PEM) fuel cell are high energy conversion efficiency, different size available, low chemical pollution, quiet operation, low running costs, and lower weight and volume than conventional batteries for electric powered vehicles. The efficiency of

* Corresponding author: kkahn@ulsan.ac.kr
1 Graduate school of Mechanical Engineering, University of Ulsan, Ulsan, Nam-gu, 44610, Korea
2 Department of Mechanical Engineering, University of Ulsan, Ulsan, Nam-gu, 44610, Korea

fuel cell hybrid excavators is also high, and it produces zero emission. Thus, fuel cell power source has gained great interest in the potential application of fuel cells to construction equipment[18-21].

Two different configurations have been proposed by Yi[18] using fuel cell-battery and Li[19-21] using fuel cell-supercapacitor. These researches used the simulation model to obtain the performance of the proposed system. However, these studies only used a simplified model of the fuel cell system and did not provide a sufficient model of the excavator. This reduces the reliability of the research results.

This paper proposes a configuration of a PEM fuel cell excavator with supercapacitor/battery hybrid power source. A fully dynamic model of the fuel cell system which deeply concerns the mechanism of the system is studied and analyzed. Supercapacitor (SC) and battery (BAT) mathematical model are also presented. These simulations are performed in MATLAB/Simulink environment. A hydraulic model of an excavator is presented, and its model is implemented in AMESim and studied. A model of the whole system is built in a co-simulation environment, which is a combination simulation of AMESim software and MATLAB/Simulink software. System working performance is also presented and discussed.

The rest of the paper is organized as follows. The proposed system is shown and discussed in Section 2. The system modeling which includes fuel cell, supercapacitor, battery model coupled with excavator hydraulic power model is presented in Section 3. Simulation results and analyses of the system performance are shown in Section 4. Conclusions are presented in Section 5.

2. System structure and principle

The proposed system structure of PEM fuel cell excavator is shown in Fig. 1. The system is divided into two parts: power sources and hydraulic excavator. The main power source PEMFC stack includes hydrogen tank, normal valve, motor, compressor, fuel cell stack, inverter and cooling system as shown in Fig. 2; supercapacitor and battery are used as the auxiliary

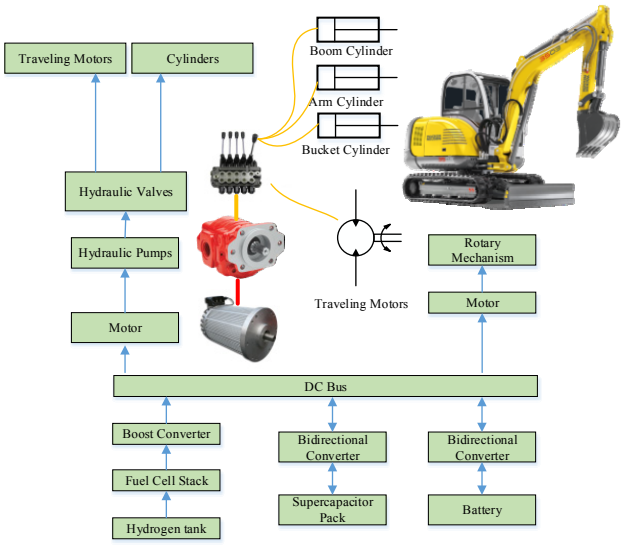

Fig. 1 System structure of PEM fuel cell excavator

energy storage devices. The FC stack cannot provide instant responses to sudden variations in the load demand of the excavator. It is the reason that the supercapacitor is used. A battery is installed to store the regenerative power produced during return action of excavator actuators or swing brake motion. Fuel cell uses hydrogen fuel and oxygen from the air to produce electricity. This energy is transferred and managed by the converter which plays the role as the brain of the system. The hydraulic system of PEM fuel cell excavator essentially involves an electric motor, a hydraulic pump, directional valves, and cylinders. The hydraulic power is supplied by the hydraulic pump driven by the electric motor. The movement of actuators is controlled by the directional valves which are received the control signal from the operator.

Fig. 2 shows the working principle of PEM fuel cell. Hydrogen fuel is supplied from the hydrogen tank to the anode, while the oxygen from the air goes to the cathode of the fuel cell stack. At the anode, a platinum catalyst causes the hydrogen to split into positive hydrogen ions and negatively charged electrons. The Polymer Electrolyte Membrane (PEM) allows only the positively charged ions to pass through it to the cathode. The negatively charged electrons must travel along an external circuit to the cathode, create an electrical current. At the cathode, the electrons and positively charged hydrogen ions combine with oxygen to form water, which is used for a cooling system.

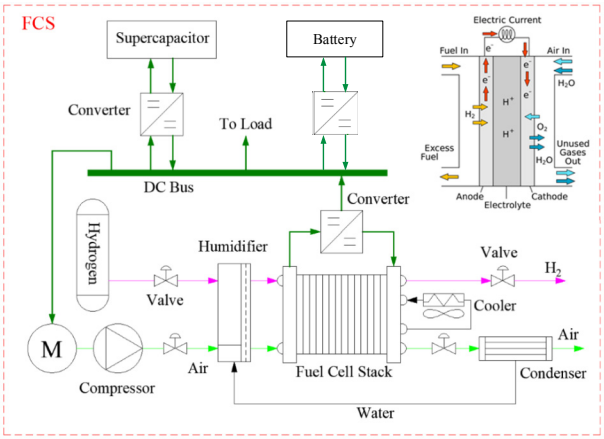

Fig. 2 Fuel Cell Stack system

3. System modeling

3.1 Supercapacitor model

The model of supercapacitor in this paper is shown as Fig. 3. A MATLAB simulation model is showed as Fig. 4[22].

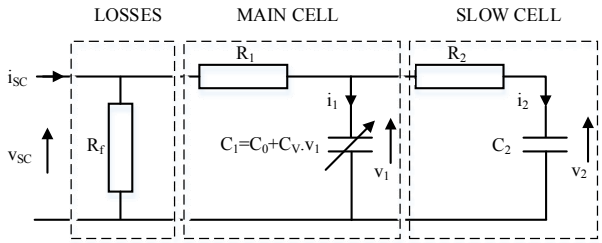

Fig. 3 Supercapacitor simplified model

The equation for circuit on Fig. 3 can be described as the following equation[22]:

$$U_{sc} = N_{s\_sc}\left(v_1 + R_1\frac{I_{sc}}{N_{p\_sc}}\right) \tag{1}$$

Where:

U_{sc} and I_{sc} are the voltage and current of the pack supercapacitor

v_{sc} and i_{sc} are the voltage and current of elementary supercapacitor

The voltage of secondary capacity C_2:

$$v_2 = \frac{1}{C_2}\int\frac{1}{R_2}(v_1 - v_2)dt \tag{2}$$

The instantaneous charge of C_2:

$$Q_2 = \int i_2 dt \tag{3}$$

The current of main capacitor:

$$i_1 = i_{sc} - i_2 \tag{4}$$

We can describe i_1 into the charge of Q_1:

$$i_1 = C_1\frac{dv_1}{dt} = \frac{dQ_1}{dt} = (C_0 + C_v v_1)\frac{dv_1}{dt} \tag{5}$$

The formula for Q_1 and v_1:

$$Q_1 = C_0 v_1 + \frac{1}{2}C_v v_1^2 \tag{6}$$

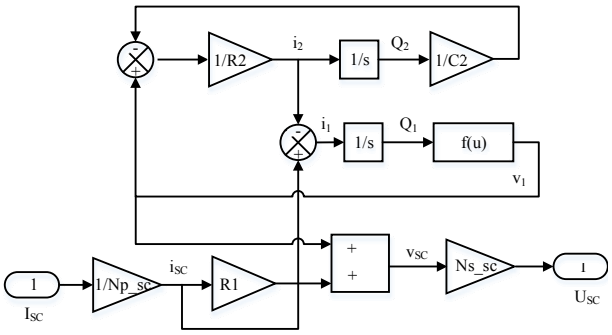

Fig. 4 MATLAB simulation model of Supercapacitors pack

3.2 Fuel cell model

- Electrochemical model

The electrochemical reactions at the anode and cathode are showed as below[23-25]:

Anode:

$$H_2 \leftrightarrow 2H^+ + 2e^- \tag{7}$$

Cathode:

$$\frac{1}{2}O_2 + 2H^+ + 2e^- \leftrightarrow H_2O \tag{8}$$

Overall:

$$H_2 + \frac{1}{2}O_2 \leftrightarrow H_2O + Heat \tag{9}$$

The output voltage of a single fuel cell can be defined by the following equation:

$$V_{cell} = E_{Nernst} - V_{act} - V_{ohmic} - V_{conc} \tag{10}$$

Where:

E_{Nernst} is thermodynamic potential

V_{act} is activation overvoltage

V_{ohmic} is the ohmic overvoltage

V_{conc} is the concentration overvoltage

The total voltage is created by combining the number of cell N as below:

$$V_{stack} = NV_{cell} \tag{11}$$

- Thermodynamic Potential

The equation for thermodynamic potential is displayed as following:

$$E_{Nernst} = E^O + \frac{RT}{nF}\ln\left[p'_{H_2}(p'_{O_2})^{0.5}\right] \tag{12}$$

Where:

E^O is the reference potential at unity activity

p'_{H_2}, p'_{O_2} represent the hydrogen and oxygen pressure, respectively

T is the cell temperature (K)

R is the universal gas constant (8.314 $Jmol^{-1}K^{-1}$)

F is Faraday constant

We can express E_{Nernst} as below:

$$E_{Nernst} = 1.229 - 8.5\times10^{-4}(T - 298.15) + \frac{RT}{2F}\ln\left[p'_{H_2}(p'_{O_2})^{0.5}\right] \tag{13}$$

- The activation overvoltage

The activation overvoltage can be described as equation following:

$$\eta_{act} = \xi_1 + \xi_2 T + \xi_3 T\left[\ln(c'_{O_2})\right] + \xi_4 T[\ln(i)] \tag{14}$$

We have four coefficients:

$$\begin{aligned}\xi_1 &= -0.948\\ \xi_2 &= 0.00286 + 0.0002\ln(A) + 4.3\times10^{-5}\ln(c'_{H_2})\\ \xi_3 &= 7.6\times10^{-5}\\ \xi_3 &= -1.93\times10^{-4}\end{aligned} \tag{15}$$

The following equations can be used for the reaction concentrations at the electrodes:

$$c'_{O_2} = p'_{O_2}\times1.97\times10^{-7}\exp\left(\frac{498}{T}\right) \tag{16}$$

$$c'_{H_2} = p'_{H_2}\times9.174\times10^{-7}\exp\left(\frac{-77}{T}\right) \tag{17}$$

The derivation of a positive term is:

$$V_{act} = -\eta_{act} \tag{18}$$

$$R_{act} = \frac{V_{act}}{i} \tag{19}$$

$$\frac{dV_{act}}{dt} = \frac{i}{C_{dl}} - \frac{V_{act}}{R_{act}C_{dl}} \tag{20}$$

With C_{dl} is the double layer capacitance of a single cell

- The ohmic overvoltage

The ohmic overvoltage of the system is calculated as the following equation:

$$V_{ohmic} = iR_{int} \tag{21}$$

With R_{int} is the internal resistance of electrolyte membrane

Or we can describe the equation (21) by using $r_M(\Omega m)$ is the membrane resistivity and l_{mem} is the thick ness of membrane (cm):

$$R_{int} = \frac{r_M l_{mem}}{A} \tag{22}$$

In this case, we can use:

$$r_M = \frac{181.6\left[1+0.03\left(\frac{i}{A}\right)+0.062(\frac{T}{303})^2(\frac{i}{A})^{2.5}\right]}{\left[\lambda-0.634-3(\frac{i}{A})\right]\exp\left[4.18\left(\frac{T-303}{T}\right)\right]} \tag{23}$$

- The concentration overvoltage

The concentration overvoltage is calculated as:

$$V_{conc} = \frac{RT}{nF}\ln\left(\frac{(i/A)_L}{(i/A)_L-(i/A)}\right) \tag{24}$$

- The reactant flow model

The reactant flow model for anode is given by the following equation:

$$\frac{V_a}{RT}\frac{dp'_{H_2}}{dt} = \dot{m}_{H_2,in} - \dot{m}_{H_2,out} - \dot{m}_{H_2,used} \tag{25}$$

With $V_a, \dot{m}_{H_2,in}, \dot{m}_{H_2,out}$ are the anode volume, hydrogen inlet, and hydrogen outlet flow-rates through fuel cell stack. Or we can use a similar equation:

$$\frac{V_a}{RT}\frac{dp'_{H_2}}{dt} = \dot{m}_{H_2,in} - \dot{m}_{H_2,out} - \frac{Ni}{2F} \tag{26}$$

We can modify (30) by using k_a is the flow constant for the anode as below:

With:

$$\dot{m}_{H_2,out} = k_a\left(p'_{H_2} - p_{\tan nk}\right) \tag{27}$$

Similar to cathode, we have:

$$\frac{V_c}{RT}\frac{dp'_{O_2}}{dt} = \dot{m}_{O_2,in} - \dot{m}_{O_2,out} - \dot{m}_{O_2,used} \tag{28}$$

With $V_a, \dot{m}_{O_2,in}, \dot{m}_{O_2,out}$ are the anode volume, hydrogen inlet, and oxygen outlet flow-rates through fuel cell stack

$$\frac{V_c}{RT}\frac{dp'_{O_2}}{dt} = \dot{m}_{O_2,in} - \dot{m}_{O_2,out} - \frac{Ni}{4F} \tag{29}$$

And:

$$\dot{m}_{O_2,out} = k_c\left(p'_{O_2} - p_{BPR}\right) \tag{30}$$

The total power input of the system:

$$P_{tot} = \dot{m}_{H_2,used}\Delta H = \frac{Ni}{2F}\Delta H \tag{31}$$

We have ΔH is the enthalpy of combustion for hydrogen

And the electrical output is:

$$P_{elec} = V_{stack} i \tag{32}$$

3.3 Battery model

The controlled voltage source is described by[26]:

$$E = E_0 - K\frac{Q_{\max}}{Q_{\max}-it} + Ae^{(-Bit)} \tag{33}$$

The battery voltage:

$$V_{batt} = E - Ri \tag{34}$$

The charge stored in battery:

$$Q = Q(t_0) - \int_{t_0}^{t} id\tau \tag{35}$$

The battery power:

$$P_{batt} = V_{batt} i \tag{36}$$

The state of charge of the battery:

$$SOC = \frac{Q}{Q_{\max}} \tag{37}$$

3.4 Excavator hydraulic model

The outlet pressure and flow rate of the hydraulic pumps can be used to calculate the demand power of the hydraulic system P_p, as follows:

$$P_p = \frac{p_i(t) q_i n_i(t)}{60 \eta_i(t)} \tag{38}$$

Where p_i, q_i, n_i, and η_i denote the pressure, displacement, efficiency, and rotational speed of the hydraulic pump, respectively. The energy-balance equations are established for the electrical motors considering their operational efficiency. The demand power of the electric motor can be estimated as follows:

$$P_M = \frac{P_p}{\eta_M} \tag{39}$$

Where P_M is the power demand of the motor driving the hydraulic pump; η_M denotes the working efficiency of the motor.

4. Simulation results and discussion

In this section, some simulations are described to show the power combination between PEM fuel cell and supercapacitor supply for a required power in a working cycle of the excavator. These simulations are implemented by using a co-simulation between AMESIM 15.2 and MATLAB 2017a with a sampling time of 10ms. The co-simulation structure which is shown in Fig. 5 includes two parts: one is the hydraulic part, and other is the power source part which includes

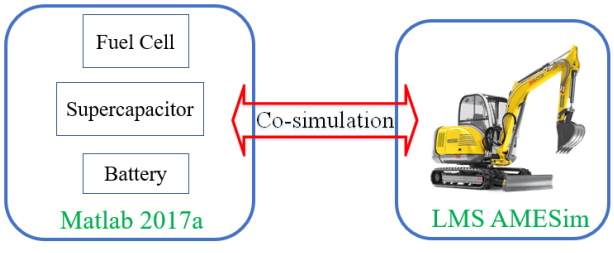

Fig. 5 Co-simulation structure

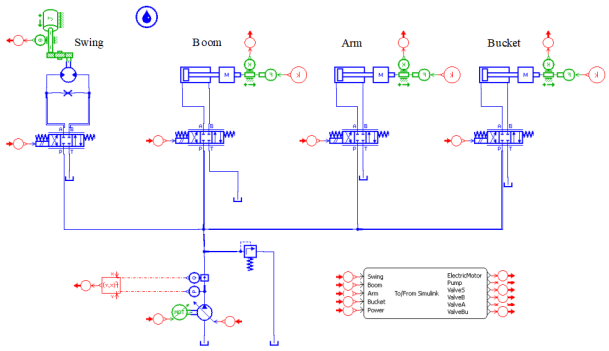

Fig. 6 Excavator AMESim hydraulic model

PEM fuel cell, battery and supercapacitor. In the system dynamics group, an S-function block is used to import the excavator dynamics which is set up in the AMESIM 15.2 as presented in Fig. 6.

The movement simulation of excavator is carried out in a working cycle. First, the arm cylinder moves down to stretch the dipper and the bucket cylinder lifts the tipping to prepare for the digging process. Next, the boom cylinder moves down the arm to touch the objective. The bucket cylinder is extended to dig the ground. After that, the boom cylinder moves up to lift the load out of the original position. The swing system will rotate the system to the new place where the excavator can shed the load. After unloading, the swing rotates to return to the previous position. The arm cylinder moves up to return the dipper to the first position. The trajectory simulation of the excavator is shown in Fig. 7. In the working process, the excavator does a lot of motions which depend on the requirement of the operators. Hence, this paper only chooses an example motion of excavator in a working cycle. Based on this trajectory simulation, the required power is estimated by AMESim simulation and shown in Fig. 8. With this result, the parameters of PEMFC, supercapacitor and battery are designed to choose exactly the size of each component. The parameters of the PEM fuel cell used in the simulation are described in Table 1-3. The parameters of the real excavator applied to simulation model are presented in Table 4.

According to Fig. 8, the performance of the total required power (P_{total}) varies depending on the tasks requested (for instance at the 5th second, the arm starts moving that requires the system power to switch from a low power to a very high power in a very short time).

Table 1: Fuel cell system parameters

Parameter	Value
Rated power, P_{rated}	5 kW
Number of cells, N	35
Cell area, A	232 cm^2
Membrane thickness, l_{mem}	178 μm
Anode pressure, P_{tank}	3 atm
Cathode pressure, P_{BPR}	3 atm

Table 2: Fuel cell model parameters

Symb.	Parameter	Value	Unit
E^O	Reference potential at unity activity	1.229	V
R	Universal gas constant	8.314	$Jmol^{-1}K^{-1}$
F	Faraday constant	96,485	$Cmol^{-1}$
C_{dl}	Double layer capacitance	0.035 x 232	F
λ	Membrane resistivity parameter	12.5	-
$(i/A)_L$	Limit current density	1.3	Acm^{-2}

Table 3: Parameters for the reactant flow models

Symb.	Parameter	Value	Unit
V_a	Anode volume	0.005	m_3
k_a	Anode flow constant	0.065	$mols^{-1}atm^{-1}$
V_c	Cathode volume	0.01	m^3
k_c	Anode flow constant	0.065	$mols^{-1}atm^{-1}$
p_{tank}	Hydrogen pressure at the inlet	3	atm
P_{BPR}	Oxygen pressure at the outlet	3	atm

Table 4: Parameters for the excavator model

Component	Value	Unit
Boom cylinder (Piston dia.*Rod dia.*Stroke length)	0.1*0.08*2	m
Arm cylinder	0.08*0.064*1.5	m
Bucket cylinder	0.063*0.042*0.5	m
Hydraulic motor (Displacement)	75	cc/rev
Hydraulic pump	100	cc/rev

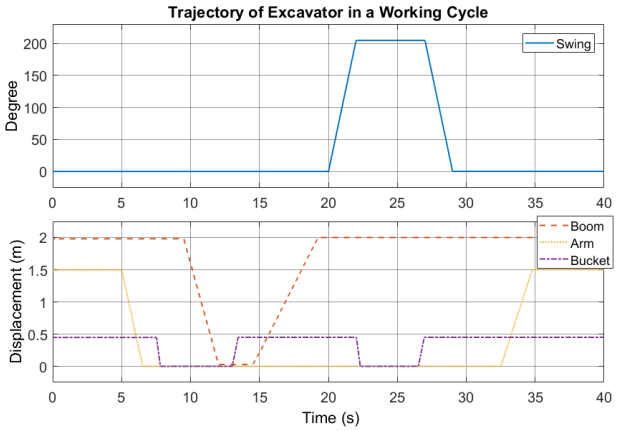

Fig. 7 Excavator trajectory of swing, boom, arm and bucket

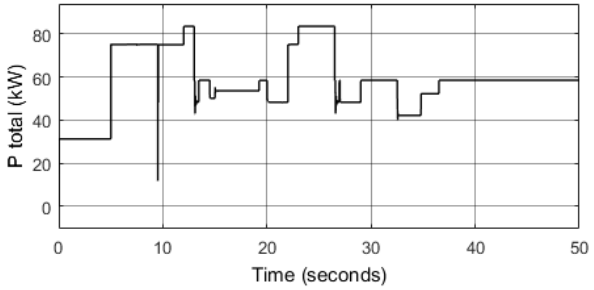

Fig. 8 Required power of the excavator

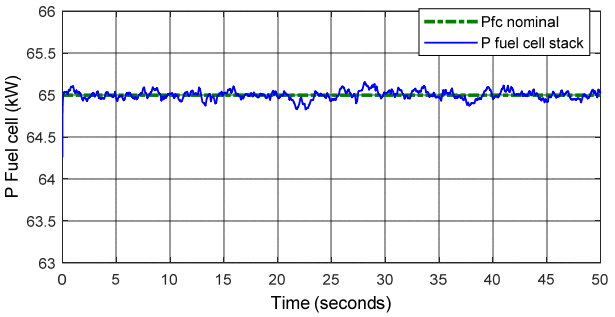

Fig. 9 Fuel cell required power and simulated output power

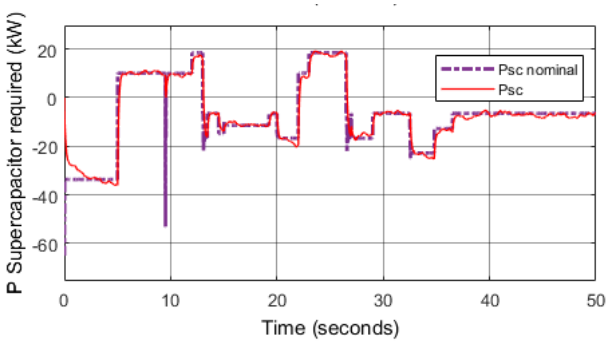

Fig. 10 Supercapacitor required power

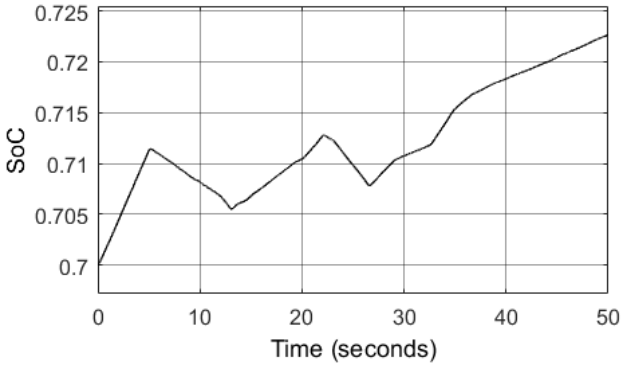

Fig. 11 Supercapacitor state of charge

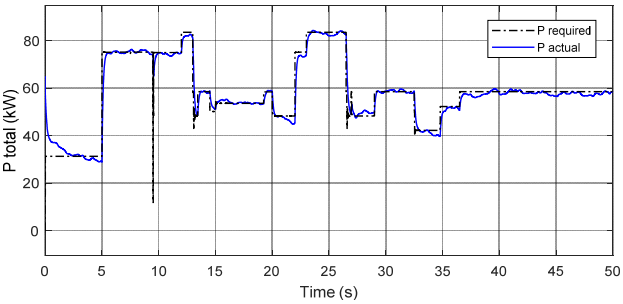

Fig. 12 Total power of fuel cell and supercapacitor

We suppose that the fuel cell (FC) can provide nominal of power at 65 kW. As can be seen in Fig. 9, the dash-dot line indicates the nominal power reference, and the rest one is for the maximum simulated power supplied by the FC. The energy losses between the reference and the simulated power in the FC due to the structure, temperature fluctuation, humidifier, and pressure during operation. In the first of 5 seconds, the power required from the excavator is less than the power supplied from the FC, then an excess power is used to charge the SC. As the necessary power exceeds the capacity of the FC at the 5th second, the SC enters the system and boosts the excavator to finish its tasks. The performance of the supercapacitor (SC) is described in Fig. 10. The dash-dot line represents for the SC required power (extracted from the difference between the P_{total} and P_{FC_n}) and the solid line is for the power generated from the SC. Positive values indicate that the SC is in discharging mode and releasing power to the excavator, whereas negative value is charging mode and storing energy. The supercapacitor state of charge (SoC_{SC}) during performing is depicted in Fig. 11. Corresponding to the performance of the power supercapacitor (P_{SC}), the SoC_{SC} increases when receiving more energy from the fuel cell and decreases when releasing energy to the excavator. The total power of fuel cell and supercapacitor is shown in Fig. 12. As shown in this figure, the actual power can track the required value. This validates the effect of the proposed system.

5. Conclusion

This paper proposed a novel design of the PEM fuel cell excavator with supercapacitor/battery hybrid power source as a method to improve excavator efficiency and cut down to zero the greenhouse emission. The dynamic model of PEM fuel cell, supercapacitor and battery is presented and discussed. The hydraulic model of the excavator is also presented. Based on these models, a co-simulation of the whole system is implemented. The simulation results validate the performance of the proposed system. Future works will consider the control aspect of the system and energy management strategy for improving efficiency and reducing fuel consumption.

Acknowledgement

This work was supported by the National Research Foundation of Korea(NRF) grant funded by the Korea government(MSIT) (No. 2017R1A2B3004625).

References

1) N. Daher, M. Ivantysynova, “Energy analysis of an original steering technology that saves fuel and boosts efficiency,” Energy Conversion and Management, Vol. 86, pp.1059 – 68, 2014.
2) T. A. Minav, L. I. E. Laurila and J.J. Pyrhonen, “Analysis of electro-hydraulic lifting system's energy efficiency with direct electric drive pump control,” Automation in Construction, Vol.30, pp.144-150, 2013.
3) D. Y. Wang and Y. Zhang, "Research on the Energy Recovery of the Excavator Slewing System Based on Hybrid Technology", Advanced Materials Research, Vol. 986-987, pp. 952-955, 2014.
4) S. Hui et al., “Control strategy of hydraulic/electric

synergy system in heavy hybrid vehicles," Energy Conversion and Management, Vol.52, pp.668–674, 2011.

5) D. Das et al., "A Novel Energy Recuperation System for Hybrid Excavator using Hybrid Actuator", 15th International Conference on Control, Automation and Systems, pp.1930-1935, 2015.
6) H. G. Park, S. A. Nahian and K. K. Anh, "A Study on Energy Saving of IMV Circuit Using Pressure Feedback", Journal of Drive and Control, Vol.13, No.4, pp.31-44, 2016.
7) H. Sun et al., "Control strategy of hydraulic/electric synergy system in heavy hybrid vehicles", Energy Conversion and Management, Vol.52, No.1, pp.668-674, 2011.
8) K. K. Ahn, T. H. Ho and Q. T. Dinh, "A study on energy saving potential of hydraulic control system using switching type closed loop constant pressure system", Proceedings of the JFPS International Symposium on Fluid Power, pp.317-322, 2008.
9) K. K. Ahn and Q. T. Dinh, "Development of energy saving hybrid excavator using hybrid actuator", Proceedings of the Seventh International Conference on Fluid Power Transmission and Control (ICFP 2009), pp. 205-209, 2009.
10) T. H. Ho and K. K. Ahn, "Saving energy control of cylinder drive using hydraulic transformer combined with an assisted hydraulic circuit", ICCAS-SICE, pp. 2115-2120, 2009.
11) K. K. Ahn and Y. Ji, "Development of Hybrid Excavator for Regeneration of Boom Potential Energy", Journal of Drive and Control, Vol.7, pp.25-32, 2010.
12) E. J. Jeong, B. M. Seo and K. K. Ahn, "Review of Energy Saving Technology of Hybrid Construction Machine," Journal of Drive and Control, Vol.15, No.3, pp.73-79, 2018.
13) Y. X. Yu, E. J. Jeong and K. K. Ahn, "Review of Energy Saving Technology of Hybrid Construction Machine," Journal of Drive and Control, Vol.15, No.4 pp.91-100, 2018.
14) C. H. Lee, "Research Trend of Autonomous Construction Machinery," Journal of Drive and Control, Vol.15, No.3, pp.68-74, 2018.
15) Volvo construction Equipment. The shape of things to come. 2018. https://www.volvoce.com/-/media/volvoce/global/global-site/this-is-volvo-ce/brochures/sfinx.pdf?v¼e5gxPw.
16) H. Steve, Scandinavia is home to heavy-duty electric construction equipment & truck development. 2018. https://cleantechnica.com/2018/01/30/scandinavia-home-heavy-duty-electric-construction-equipment-truckdevelopment/.
17) Symbio. ELEXC 2019. https://www.symbio.one/en/elexc-2/.
18) H. Yi et al., "Optimal Component Sizing of Fuel Cell-Battery Excavator Based on Workload," International Journal of Precision Engineering and Manufacturing-Green Technology, Vol.5, pp.103-110, 2018.
19) T. Li et al., "Design and analysis of a fuel cell supercapacitor hybrid construction vehicle," Int. J. Hydrogen Energy, Vol.41, pp.12307-12319, 2016.
20) T. Li, H. Liu and D. Ding, "Predictive energy management of fuel cell supercapacitor hybrid construction equipment," Energy, Vol.149, pp.718-729, 2018.
21) T. Li, L. Huang and H. Liu, "Energy management and economic analysis for a fuel cell supercapacitor excavator," Energy, Vol.172, pp. 840-851, 2019.
22) A. Lahyani et al., "Battery/Supercapacitors Combination in Uninterruptible Power Supply (UPS)," IEEE Transactions on Power Electronics, Vol.28, pp.1509-1522, 2013.
23) M. Khan and M. Iqbal, "Modelling and Analysis of Electro chemical, Thermal, and Reactant Flow Dynamics for a PEM Fuel Cell System," Fuel Cells, Vol.5, pp.463-475, 2005.
24) K. Sankar, K. Aguan and A. Jana, "A proton exchange membrane fuel cell with an airflow cooling system: Dynamics, validation and nonlinear control," Energy Conversion and Management, Vol.183, pp.230-240, 2019.
25) F. Musio et al., "PEMFC system simulation in MATLAB-Simulink® environment," International Journal of Hydrogen Energy, Vol.36, pp.8045-8052, 2011.
26) O. Tremblay, L. Dessaint and A Dekkiche, "A Generic Battery Model for the Dynamic Simulation of Hybrid Electric Vehicles," IEEE Vehicle Power and Propulsion Conference, 2007.